# A $Ca^{2+}$-Binding Domain in RyR1 that Interacts with the Calmodulin Binding Site and Modulates Channel Activity

Liangwen Xiong, Jia-Zheng Zhang, Rong He, and Susan L. Hamilton
Department of Molecular Physiology and Biophysics, Baylor College of Medicine, Houston, Texas

ABSTRACT A fragment of RyR1 (amino acids 4064–4210) is predicted to fold to at least one lobe of calmodulin and to bind $Ca^{2+}$. This fragment of RyR1 (R4064–4210) was subcloned, expressed, refolded, and purified. Consistent with the predicted folding pattern, R4064–4210 was found to bind two molecules of $Ca^{2+}$ and undergo a structural change upon binding $Ca^{2+}$ that exposes hydrophobic amino acids. R4064–4210 also binds to RyR1, the L-type $Ca^{2+}$ channel ($Cav_{1.1}$), and several synthetic calmodulin binding peptides. Both R4064–4210 and a peptide representing the calmodulin-binding region of RyR1 (R3614–3643) alter the $Ca^{2+}$ dependence of ($^3$H)ryanodine binding to RyR1, suggesting that they may both be interfering with an intramolecular interaction between amino acids 4064–4210 and amino acids 3614–3643 in the native RyR1 to alter or regulate the response of the channel to changes in $Ca^{2+}$ concentration. The finding that a domain within RyR1 binds $Ca^{2+}$ and interacts with calmodulin-binding motifs may provide insights into the mechanism for calcium- and calmodulin-dependent regulation of this channel and perhaps for its regulation by the L-type $Ca^{2+}$ channel.

## INTRODUCTION

$Ca^{2+}$ release channels, also known as ryanodine receptors (RyRs), regulate the release of $Ca^{2+}$ from sarcoplasmic reticulum (SR) stores. The released $Ca^{2+}$ triggers muscle contraction and activates a cascade of $Ca^{2+}$-dependent signal transduction pathways. $Ca^{2+}$ and calmodulin (CaM) are important as in vivo modulators of RyRs. RyR1 activity displays a bell-shaped dependence on $Ca^{2+}$ concentration, with enhancement of channel activity in the low $\mu$M range, but inhibition of the channel in the high $\mu$M to mM range (1,2). Several motifs within the primary amino-acid sequence of RyRs have been suggested to resemble $Ca^{2+}$-binding E-F hand motifs in $Ca^{2+}$-binding proteins (3,4). Putative E-F hands have been identified in RyR1 at amino acids 4253–4264, 4407–4416, and 4489–4499 (5), in RyR2 at amino acids 1136–1347 and 2010–2021 (6), and in RyR3 at amino acids 3934–3945 (7). Fragments of RyR1 containing some of these E-F hand motifs have been shown to bind $Ca^{2+}$ (8–10). The low-affinity inhibitory $Ca^{2+}$ binding site was suggested to be within the negatively charged region between residues 1872–1923 (11,12); however, the replacement of this glutamate-rich sequence with the corresponding, less-acidic sequence from RyR2 did not change low-affinity $Ca^{2+}$ inactivation of RyR1 (12). Du and MacLennan suggested that the $Ca^{2+}$ binding sites for both activation and inactivation of RyR1 are located at the C-terminus between residues 3726 and 5037 (13). This region has three potential E-F hands (5) and several other possible $Ca^{2+}$-binding sequences (14–16). Mutation of some amino acids in this region alters $Ca^{2+}$ binding and $Ca^{2+}$ regulation of RyR1 (17). To determine if any of these putative E-F hands are involved in $Ca^{2+}$ regulation of the channel, Fessenden et al. (18) created mutant RyRs in which the putative E-F hands were scrambled either singly or in combination with other E-F hands. These investigators found that, in intact myotubes, the mutations did not affect functional responses to depolarization, caffeine, or 4-chloro-m-cresol (4-CmC) (18). However, ($^3$H)ryanodine binding and its $Ca^{2+}$ dependence were altered by the E-F-1 mutations and abolished by the E-F-2 mutations, suggesting an involvement of these E-F hands in $Ca^{2+}$ regulation of the channel. Why would this be different in the myotubes? One possibility is that a $Ca^{2+}$-binding protein such as CaM, which can itself both activate and inhibit the channel in a $Ca^{2+}$-dependent manner, can override the need for $Ca^{2+}$ binding directly to the channel in the myotubes. This unanswered question emphasizes the need for further investigation.

CaM can function as either an activator or an inhibitor of RyR1, depending on whether it has $Ca^{2+}$ bound (19). At sub-$\mu$M $Ca^{2+}$ concentrations, CaM is an activator of RyR1, but at higher $Ca^{2+}$ concentrations, it becomes an inhibitor (19–21). Both $Ca^{2+}$-free and $Ca^{2+}$-bound CaMs bind to RyR1 at a site close to amino acids 3614–3643 (22,23). This sequence is likely to represent the binding site for the C-lobe of CaM (24), whereas the N-lobe may bind to an adjacent subunit within the RyR1 tetramer between amino acids 1975 and 1999 (25). We previously have shown that a carboxy-terminal tail fragment of the skeletal L-type channel ($Ca_v1.1$) $\alpha_1$-subunit, which contains both $Ca^{2+}$ and CaM binding sites, binds to RyR1. This interaction is blocked by $Ca^{2+}$CaM (26). We have also shown that a peptide representing the CaM binding site on RyR1 (amino acids 3614–3643) binds to both the $Ca_v1.1$ and an expressed fragment of the carboxy-terminal tail of its $\alpha_1$-subunit (amino acids 1393–1527) (26).

*Submitted May 11, 2005, and accepted for publication September 27, 2005.*

Address reprint requests to Susan L. Hamilton, Dept. of Molecular Physiology and Biophysics, Baylor College of Medicine, 1 Baylor Plaza, Houston, TX 77030. Tel.: 713-798-3894; Fax: 713-798-5441; E-mail: susanh@bcm.tmc.edu.



0006-3495/06/01/173/10 $2.00

doi: 10.1529/biophysj.105.066092

The interaction of R3614–3643 with the $Ca_v1.1$ is also blocked by $Ca^{2+}$ CaM (26). Three sequences on the carboxy-terminal tail of the cardiac L-type $Ca^{2+}$ channel ($Ca_v1.2$), designated *A* (1609–1628, numbering of the human cardiac channel), *C* (1627–1652), and *IQ* (1665–1685) have been implicated in CaM binding (27–30). Synthetic peptides matching these sequences or their skeletal muscle counterparts do not interact with R3614–3643 (unpublished observation), suggesting that there is another site within $Ca_v1.1$ that can bind to R3614–3643.

Since the CaM binding domains on $Ca_v1.1$ and RyR1 do not directly interact, we began to search for other interaction sites. Using 3D-PSSM (http://www.sbg.bio.ic.ac.uk), we identified a sequence within RyR1 (amino acids 4064–4210) and one within the carboxyterminal tail of the $Ca_v1.1$ $\alpha_1$-subunit (amino acids 1395–1540) predicted to fold like CaM and bind $Ca^{2+}$. One possibility is that these CaM-like domains can interact with the CaM binding sites of these proteins and CaM would compete for this interaction. To assess this possibility, we expressed the CaM-like domain of RyR1 and examined its ability to bind $Ca^{2+}$and to interact with RYR1, the L-type channel, and several CaM-binding peptides. (See Table 1 for a list of all peptides used.)

## EXPERIMENTAL PROCEDURES

### Materials

The peptides were synthesized in the core facility at Baylor College of Medicine (Houston, TX) under the direction of Dr. Richard Cook. SR membranes were prepared from rabbit hind leg and backstrap skeletal muscle as previously described (31). Protein concentrations were determined by the Lowry method (32) using bovine serum albumin as the standard. ($^3$H)ryanodine (70–80 Ci/mmol) was purchased from Du Pont New England Nuclear (Boston, MA); unlabeled ryanodine was purchased from Calbiochem (La Jolla, CA).

### Creation of the construct for expressing R4064–4210

To subclone the fragment of RyR1 cDNA coding for the region of RyR1 predicted to fold like CaM, we used PCR primers containing *Nde*I and *Hin*dIII restriction sites, with a stop-codon in the reverse primer. PCR reactions amplified the desired DNA fragment by selective priming of the full-length rabbit skeletal RyR1 cDNA. The amplified PCR products were agarose gel-purified and then ligated into pCR-Blunt vector (Invitrogen, San Diego, CA). The ligates were transformed into One-Shot TOP-10 Competent Cells (Invitrogen) for amplification. After confirmation by DNA sequencing, the desired DNA fragments were excised using the enzymes whose restriction sites were pre-incorporated into primers. The released DNA fragment was subcloned into pET23a(+) or pET28a(+) vectors (Novagen, Madison, WI) between *Nde*I and *Hin*dIII sites. The subcloned products were transformed into DH5$\alpha$ competent cells (Invitrogen) to amplify. DNA sequencing was performed again for verification of the desired DNA sequences in the expression vectors.

**TABLE 1 Peptides used in this study**

| | |
|---|---|
| R4064–4210 | MFLKLKD IVGSEAFQDYVTDPRGLISK KDFQKAMDSQKQF TGPEIQFLLSCSEADENEMINFEEFAN RFQEPARDIGFNVAV LLTN LSEHVPHDPRLRNFLELAESI LEYFRPYLGRIEIMGAS RRIERIYF EISETNRAQWEMPQV |
| R3614–3627 | KSKKAVWHKLLSKQ |
| R3614–3634 | KSKKAVWHKLLSKQRRRAVVA |
| R3614–3643 | KSKKAVWHKLLSKQRRRAVVACFRMTPLYN |
| R3625–3644 | SKQRRRAVVACFRMTPLYNL |
| Skeletal IQ | KFYATFLIQEHFRKFMKRQEE |
| C-peptide | EQANEELRAIIKKIWKRTSMKLLDQV |
| CaMKII peptide | MHRQEAVDCLKKFNARRKLKG |

### Expression, purification, and refolding of R4064–4210

The expression vectors containing the DNA construct for R4064–4210 were transformed into BL21(DE3) competent cells (Novagen). The fragment R4064–4210 was found almost exclusively in inclusion bodies when expressed either with or without a 20-amino acid His tag (MGSSHHHHHHSSGLVPRGSH) at the N-terminus of the fragment (in pET28a(+) or pET23a(+) vector). To purify this fragment from inclusion bodies, the cytoplasmic proteins were first extracted using Bacterial Protein Extraction Reagent (B-PER; Pierce Biotechnology, Rockford, IL) and then the bacterial membrane proteins were extracted by B-PER Bacterial Protein Extraction Reagent with lysozyme and nuclease. The remaining insoluble material, which is greatly enriched in R4064–4210, was washed with inclusion body wash buffer (50 mM Tris-HCl pH 7.4, 1% Triton or CHAPS, 5 mM DTT, and 5 mM EDTA). R4064–4210 was extracted with 50 mM Tris-HCl pH 7.4 and 2 M urea. The His-tagged protein was purified with a chelating sepharose column (Amersham Pharmacia Biotech, Piscataway, NJ) with a buffer containing 2 M urea. The chelating sepharose-purified R4064–4210 was dialyzed against 20-mM Tris-HCl pH 7.4 in a 10,000 MWCO cassette (Pierce). The dialysis buffer was changed twice to remove the urea and refold the protein. The urea-extracted untagged protein was refolded in a manner similar to the His-tagged protein and purified by anion exchange (HiTrap Q HP) and phenyl sepharose chromatography (Amersham Pharmacia Biotech).

### Circular dichroism spectroscopy

To demonstrate the refolding of R4064–4210, circular dichroism (CD) spectroscopy was used to analyze its secondary structure. Untagged R4064–4210 (0.1 mg/ml) was incubated in 5 mM Tris-HCl pH7.9, 1 mM EGTA, or 1 mM $Ca^{2+}$ for 10 min at room temperature. CD spectra were recorded on an Aviv CD instrument, Model #62A DS (Aviv, Lake Wood, NJ) from 188 to 250 nm with 1 nm/step, using a 2-mm quartz cell. Data were processed by subtracting the CD signal of buffer/additives and by averaging the data obtained from three independent experiments.

### Analysis of $^{45}$Ca binding to R4064–4210 by equilibrium dialysis

R4064–4210 (15 $\mu$M, 100 $\mu$l) in 30 mM HEPES pH 7.0, 0.2 mM PMSF, and 5 mM $\beta$-mercaptoethanol was injected into one of two chambers of an equilibrium dialysis cell (Bel-Art Products, Pequannock, NJ), separated by a 3500 MWCO membrane. The same amount of the buffer containing different concentrations of $^{45}Ca^{2+}$ (5–200 $\mu$M, 1 $\mu$Ci/$\mu$mol) was injected into the other cell. The equilibrium dialysis cells were incubated at 20°C overnight with rotation, after which 50 $\mu$l was removed from each chamber for analysis of $^{45}Ca^{2+}$ by liquid scintillation counting. $^{45}Ca^{2+}$ bound to R4064–4210 was calculated from the difference in $^{45}Ca^{2+}$ radioactivity in the two chambers. The data were fit with a four-parameter Hill equation in SigmaPlot (SPSS, Chicago, IL).

### ANSA fluorescence analysis probes conformational changes of R4064–4210 induced by $Ca^2$

To assess the ability of the RyR1 fragment to undergo $Ca^{2+}$-induced conformational changes, we used 8-anilino-1-naphthalenesulfonic acid ammonium (ANSA) (Sigma-Aldrich, St. Louis, MO) fluorescence analysis. ANSA (1 $\mu$M) was incubated in 30 mM MOPS (pH 7.2) and either 5 mM EGTA (low $Ca^{2+}$) or 2 mM $Ca^{2+}$ (high $Ca^{2+}$) for 5 min at room temperature in the presence or absence of untagged R4064–4210 (0.4 $\mu$M). Fluorescence emission spectra from 430 to 600 nm were collected with 370-nm excitation using an ISS PC1 Photon Counting Spectrofluorometer (ISS, Champaign, IL), with a 0.5-mm slit for excitation and 2-mm slit for emission, 1 nm/step. Relative fluorescence was corrected for buffer contribution. All experiments were repeated at least three times.

### R4064–4210 binding to CaM-binding peptides by ANSA fluorescence analysis

R4064–4210 (0.5 $\mu$M) and ANSA (2 $\mu$M) were incubated in 30 mM MOPS (pH 7.2) containing 5 mM EGTA, 50 $\mu$M $Ca^{2+}$, 500 $\mu$M $Ca^{2+}$, or 5 mM $Ca^{2+}$ for 5 min at room temperature; 5 $\mu$M of different peptides (R3614–3643, C-peptide (27), CaM kinase II Inhibitor (Calbiochem) or the IQ-peptide (30)) were then added. ANSA fluorescence emission data at 470 nm were collected on an SLM 8000C Spectrofluorometer (SLM Instruments, Urbana, IL) with a 370-nm excitation, 8-nm bandpass for excitation, and 16-nm bandpass for emission. Data were processed by subtracting the background of buffer and/or additives where appropriate and the data were fit with a four-parameter Hill equation in SigmaPlot (SPSS).

### Identification of the amino acids interacting with R4064–4210

To determine which amino acids in R3614–3643 were involved in R4064–4210 binding, we used overlapping peptide fragments from amino acids 3614–3644 to interact with R4064–4210 in the presence of ANSA. R4064–4210 (0.5 $\mu$M) and ANSA (2 $\mu$M) were incubated in 30 mM MOPS (pH 7.2) containing 5 mM EGTA (low $Ca^{2+}$) or 500 $\mu$M $Ca^{2+}$ (high $Ca^{2+}$) for 5 min at room temperature. Peptides (R3614–3627, R3614–3634, R3614–3643, and R3625–3644) were then added and the ANSA fluorescence data were collected on an SLM 8000C Spectrofluorometer (SLM Instruments).

### The effect of R4064–4210 and synthetic peptides on ($^3$H)ryanodine binding

SR membranes (10 $\mu$g) were incubated with ($^3$H)ryanodine (5 nM) for 16 h at room temperature in 100 mM NaCl, 30 mM MOPS (pH7.2), 100 $\mu$g/ml BSA, and 0.1% CHAPS, containing increasing $CaCl_2$ with 10 $\mu$M different proteins or peptides. Bound radiolabel was separated from free by filtration through Whatman GF/F filters with 5 $\times$ 3 ml washes of ice cold buffer (Whatman, Brentford, Middlesex, UK). Nonspecific binding was determined in the presence of 10-$\mu$M unlabeled ryanodine.

### Assessing the interaction of R4064–4210 with $Ca_v1.1$ by pulldown assays

His-tagged R4064–4210 (3 nM) or a synthetic His tag alone were incubated with 300 $\mu$l of a Ni charged chelating sepharose bead slurry in binding buffer consisting of 50 mM MOPS (pH 7.4), 20 mM imidazole, 1 mM $CaCl_2$ (designated high $Ca^{2+}$ buffer) or 2 mM EGTA (designated low $Ca^{2+}$ buffer) for 30 min. The IQ-peptide (3 nM, sequence: KFYATFLIQEHFRKFMKRQEE) from the C-terminus of the skeletal L-type $Ca^{2+}$ channel ($Ca_v1.1$, $\alpha_1$-subunit) or digitonin-solubilized T-tubule membranes (24 $\mu$g) were added to this bead slurry. After 1-h incubation, the beads were washed twice with 300-$\mu$l binding buffer and proteins were eluted with SDS sample buffer for electrophoresis. The pulldown of the IQ-peptide by R4064–4210 was assessed by Coomassie staining of the SDS gel (in duplicate and repeated three times). $Ca_v1.1$ in the pulldown was determined by Western blotting with an anti-$Ca_v1.1$ $\alpha_{1s}$ antibody, MA3-920 (Affinity BioReagents, Golden, CO), and Alexa Fluor 680 (Molecular Probes, Eugene, OR) as secondary antibody (in triplicate and repeated twice). An Odyssey Infrared Imaging System (LI-COR, Lincoln, NE) was used to analyze the Western blots. To verify the specific interaction of R4064–4210 with $Ca_v1.1$, parallel Western blotting experiments were conducted, but with an anti-sodium/potassium ATPase $\alpha$-1 antibody, MA3-929 (Affinity BioReagents).

## RESULTS

### R4064–4210 is predicted by 3D-PSSM to fold similar to calmodulin

We have previously shown that a synthetic peptide matching the CaM binding site on RyR1 bound to $Ca_v1.1$, and, conversely, that a CaM binding peptide from $Ca_v1.1$ bound to RyR1 (26). Since the CaM binding peptides from these two channels do not themselves interact (unpublished observation), we began to look for sequences within RyR1 that could bind to the carboxy-terminal tail of the $Ca_v1.1$ $\alpha_1$-subunit. A region of $Ca_v1.1$ (amino acids 1395–1540) that contains the putative E-F hands was previously predicted by 3D-PSSM (http://www.sbg.bio.ic.ac.uk) to fold like CaM and was shown to interact with CaM binding peptides from RyR1 and $Ca_v1.1$ (26). The CaM binding peptide from RyR1 has been shown to bind both $Ca^{2+}$CaM and apoCaM (22,23). We found a region of RyR1 (amino acids 4064–4210) that was also predicted to fold in a manner similar to CaM (>95% confidence level, 21% sequence identity, Fig. 1 *A*).

### Extraction and refolding of R4064–4210 from inclusion bodies after expression in *Escherichia coli*

A fragment of RyR1 representing this putative CaM-like domain and designated R4064–4210 was expressed in BL21(DE3) cells. The protocol used for the expression generated 30–50 mg of R4064–4210 per liter of culture. The R4064–4210 was found almost exclusively in inclusion bodies but could be solubilized in 2 M urea (*lane 5* of Fig. 1 *B*). The urea-solubilized R4064–4210 was refolded by dialysis into buffer without urea and was soluble at concentrations as high as 10 mg/ml (*lane 7* of Fig. 1 *B*).

### Assessing the $\alpha$-helical content of R4064–4210

R4064–4210 appeared to be both homogenous and structured as assessed by its CD signal at both low (*solid line* of Fig. 1 *C*) and high $Ca^{2+}$ concentrations (*dashed line* of Fig. 1 *C*). There is a strong positive CD maximum at 192 nm and

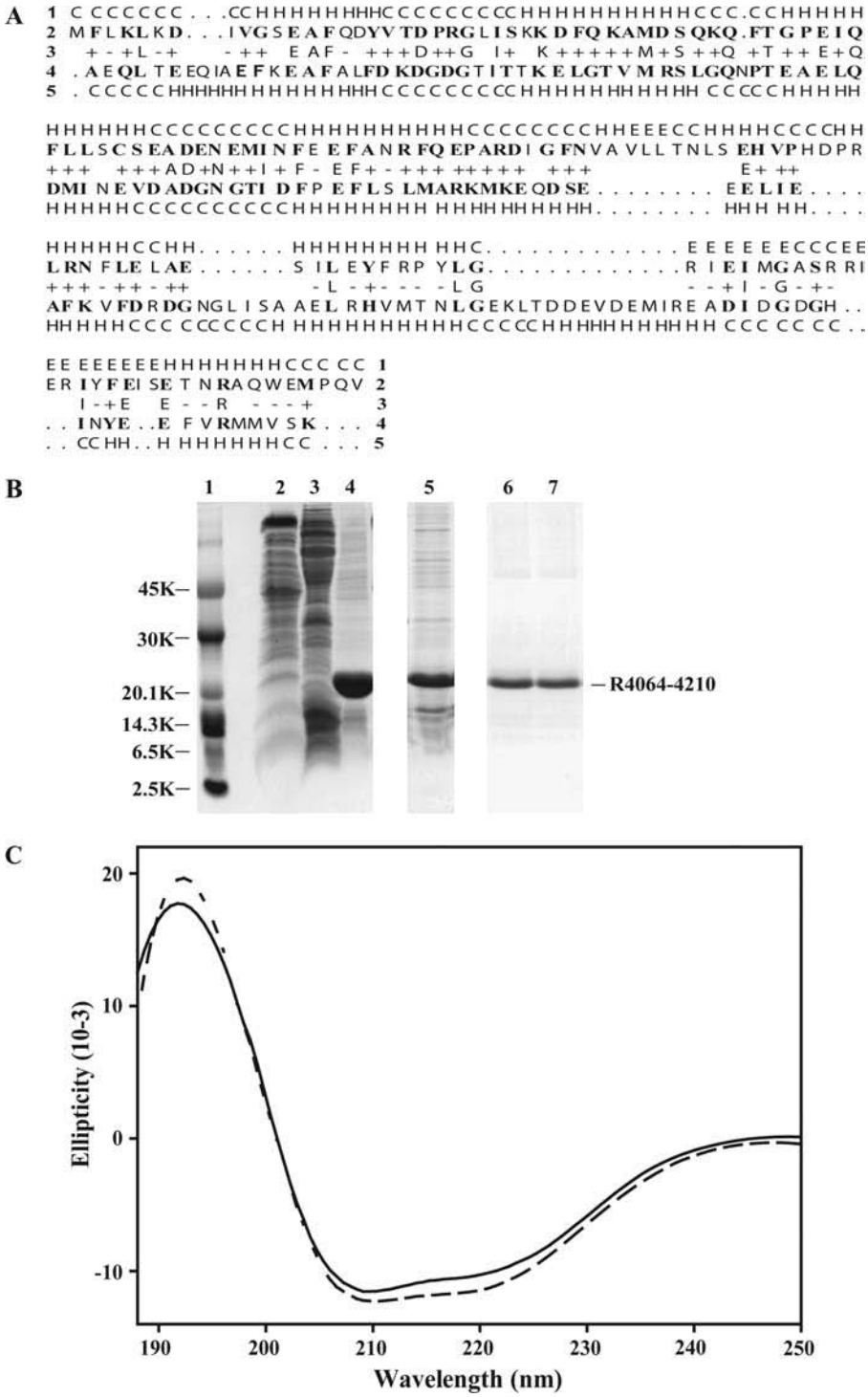


FIGURE 1 Expression, refolding, and predicted secondary structure of R4064–4210. (*A*) Secondary structural comparison of R4064–4210 with calmodulin by 3D-PSSM Fold prediction. Row *2* shows the amino-acid sequence of R4064–4210. Row *4* is the sequence of *Paramecium* CaM, found to be the best structural match to R4064–4210 in the 3D-PSSM Fold Library. The bold letters in rows *2* and *4* are identical/similar amino acids between R4064–4210 and calmodulin. Row *1* predicts the secondary structures of R4064–4210 and row *5* shows the secondary structures of *Paramecium* calmodulin found in the Fold Library (*H*, $\alpha$-helix; *E*, $\beta$-strand; and *C*, coil). Row *3* demonstrated the identity between R4064–4210 and *Paramecium* calmodulin. The letters mean that R4064–4210 and *Paramecium* calmodulin have the same amino acids in the alignment. The plus (+) versus minus (−) symbols indicate a good-versus-poor match between the sequence of R4064–4210 and *Paramecium* calmodulin, respectively. The R4064–4210 sequence was predicted to have >95% probability of folding like CaM. The overall sequence identity was 21%. (*B*) Expression, purification, and refolding of R4064–4210. The His-tagged and untagged proteins have similar expression, purity, and solubility. For simplicity, only the results for the His-tagged protein are shown. Cytoplasmic proteins were extracted by B-PER Bacterial Protein Extraction Reagent (*lane 2*), and membrane proteins were extracted by B-PER Bacterial Protein Extraction Reagent with lysozyme and nuclease (*lane 3*), and insoluble material (*lane 4*). Upon comparing the molecular size of His-tagged R4064–4210 to the markers (*lane 1*), it was found that R4064–4210 was overexpressed in the inclusion body (*lane 4*). 2 M urea extracted R4064–4210 from the inclusion body (*lane 5*). The urea-extracted materials were purified by chelating sepharose (Amersham Pharmacia Biotech) in the presence of 2 M urea for all buffers (*lane 6*). The purified R4064–4210 was refolded by dialyzing against 20 mM Tris-HCl pH7.4 (*lane 7*). (*C*) R4064–4210 is rich in $\alpha$-helical structure as assessed by CD spectroscopy. R4064–4210 (0.1 mg/ml) was incubated in 5 mM Tris-HCl (pH7.9), 1 mM EGTA (*solid line*), or 1 mM $Ca^{2+}$ (*dashed line*) for 10 min at room temperature. The CD spectra were recorded from 188 to 250 nm.

two negative CD maxima centered at 210 and 222 nm, indicative of proteins with a high $\alpha$-helical content (33). Furthermore, the high $\alpha$-helical structural content is consistent with the prediction for folding obtained with 3D-PSSM (Fig. 1 *A*). The CD spectrum of this fragment is similar to that of CaM (24). Unlike CaM, $Ca^{2+}$ produced only small changes in the $\alpha$-helical content of R4064–4210, suggesting that the structural changes in this fragment upon binding $Ca^{2+}$ are probably not as extensive as those in CaM.

## The ability of R4064–4210 to bind $Ca^{2+}$

To assess the ability of R4064–4210 to bind $Ca^{2+}$ we used micro-equilibrium dialysis with $^{45}Ca^{2+}$. We found that two

molecules of $^{45}Ca^{2+}$ bound per mol of R4064–4210 (1.9 ± 0.3 pmol $^{45}Ca^{2+}$ bound per pmol of R4064–4210, with an apparent affinity of 60 ± 12 $\mu$M, $n = 3$, and a Hill coefficient of 1.6 ± 0.4; see Fig. 2 *A*). To confirm the ability of R4064–4210 to bind $Ca^{2+}$ we also used terbium fluorescence. We found that terbium fluorescence was increased in the presence of R4064–4210 and that the increase is inhibited by $Ca^{2+}$ (data not shown), suggesting that $Ca^{2+}$ competes with terbium for a common binding site on this fragment of RyR1.

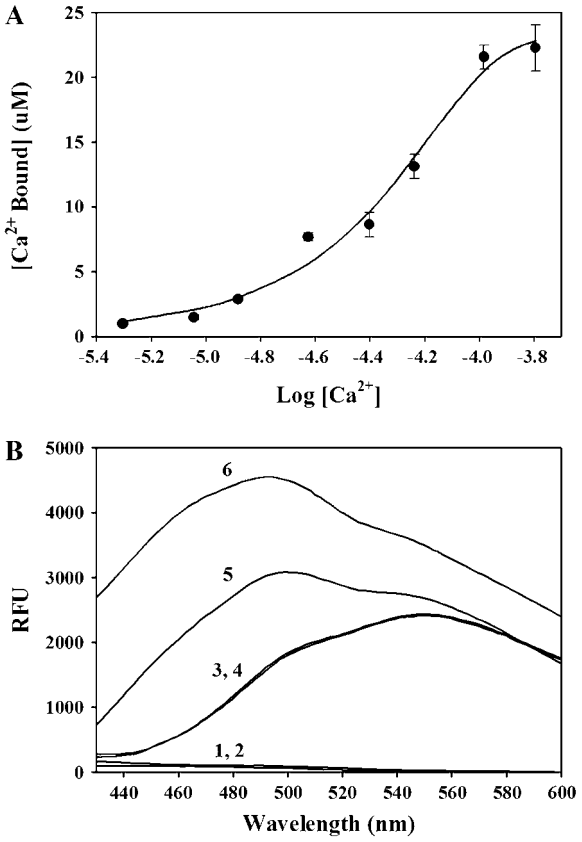


FIGURE 2 R4064–4210 binds $Ca^{2+}$. (*A*) Analysis of $^{45}Ca^{2+}$ binding to R4064–4210 by equilibrium dialysis. R4064–4210 (15 $\mu$M, 100 $\mu$l) in 30 mM HEPES pH 7.0 was injected into one of two chambers of an Equilibrium Dialysis cell, separated by a 3500-MWCO membrane. The same amount of the buffer containing different concentrations of $^{45}Ca^{2+}$ was injected into the other chamber. After overnight incubation, 50-$\mu$l aliquots were removed from each chamber for determination of $^{45}Ca^{2+}$ by liquid scintillation counting. $^{45}Ca^{2+}$ bound to R4064–4210 was determined from the difference in $^{45}Ca^{2+}$ radioactivity in the two chambers. By a four-parameter Hill fitting, R4064–4210 apparent affinity for $Ca^{2+}$ ($EC_{50}$) = 60 ± 12 $\mu$M, maximum binding ($B_{max}$) = 1.9 ± 0.3 pmol $^{45}Ca^{2+}$ bound per pmol of R4064–4210, and the Hill coefficient = 1.6 ± 0.4. (*B*) $Ca^{2+}$ binding to R4064–4210 alters ANSA fluorescence. R4064–4210 (0.4 $\mu$M) was incubated with ANSA (1 $\mu$M) in 30 mM MOPS (pH 7.2), with either 5 mM EGTA (low $Ca^{2+}$) or 2 mM $Ca^{2+}$ (high $Ca^{2+}$) for 5 min at room temperature. Fluorescence emission spectra from 430 to 600 nm were collected with a 370-nm excitation wavelength. *1*, R4064–4210 (low $Ca^{2+}$); *2*, R4064–4210 (high $Ca^{2+}$); *3*, ANSA (low $Ca^{2+}$); *4*, ANSA (high $Ca^{2+}$); *5*, R4064–4210 + ANSA (low $Ca^{2+}$); and *6*, R4064–4210 + ANSA (high $Ca^{2+}$).

## $Ca^{2+}$-induced changes in R4064–4210 assessed by ANSA fluorescence probe analysis

To determine if R4064–4210 undergoes a structural change upon binding $Ca^{2+}$, we used ANSA, a probe that increases its fluorescence when bound to the hydrophobic sites on proteins (34). We found that $Ca^{2+}$ increased ANSA fluorescence in the presence of R4064–4210 (Fig. 2 *B*), suggesting that $Ca^{2+}$ binds to R4064–4210 and induces exposure of hydrophobic regions.

## R4064–4210 binds to the CaM binding motif (R3614–3643) of RyR1

R4064–4210 binds directly to a peptide (R3614–3643) representing the CaM binding site on RyR1. We found a very dramatic increase in ANSA fluorescence with increasing concentrations of R3614–3643 (Fig. 3). If the R4064–4210 region of RyR1 is important for $Ca^{2+}$-dependent regulation of RyR1 activity, the interactions should be in some way regulated by the binding of $Ca^{2+}$. To assess this, we examined the interaction of R3614–3643 with R4064–4210 at different $Ca^{2+}$ concentrations (Fig. 3). We found that R3614–3643 apparently interacts with R4064–4210 at the all of the $Ca^{2+}$ concentrations tested, but that the affinity and the apparent magnitude of the ANSA fluorescence changes were different at different $Ca^{2+}$ concentrations. The apparent affinities of R3614–3643 for R4064–4210 at <10 nM, 50 $\mu$M $Ca^{2+}$, 500 $\mu$M $Ca^{2+}$, and 5 mM $Ca^{2+}$ were 803 ± 47 nM, 230 ± 7 nM, 268 ± 8 nM, and 181 ± 10 nM, respectively. The magnitude of the ANSA fluorescence change was also different at the different $Ca^{2+}$ concentrations, with the smallest change occurring at 5 mM and <10 nM $Ca^{2+}$ (concentrations where RyR1 is less active). An interaction of the CaM-like domain (R4064–4210) at both high and low $Ca^{2+}$ concentrations is consistent with R3614–3643 being a binding site for both apoCaM and $Ca^{2+}$CaM (22,23).

## Amino-acid determinants in R3614–3643 required for R4064–4210 binding

To determine which amino acids within the CaM binding site of RyR1 were required for the interaction with R4064–4210, we tested the ability of a series of overlapping peptides from this region for the ability to interact with R4064–4210 using ANSA fluorescence to assess the interactions. We found that a peptide corresponding to amino acids 3614–3634 (*solid circles* in Fig. 4 *A*) had an apparent affinity ($EC_{50}$ = 251 ± 17 nM) that was similar to R3614–3643 (268 ± 8 nM) (*solid squares* in Fig. 4 *A*) at high $Ca^{2+}$; however, the magnitude of the fluorescence change induced by R3614–3634 was much less than that induced by R3614–3643. This finding suggests that determinants between amino acids 3614–3634 were important for affinity, but that determinants between amino acids 3635 and 3643 are needed to induce the conformational

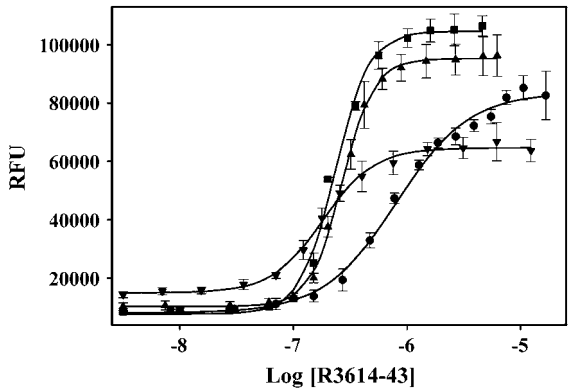


FIGURE 3 R4064–4210 interaction with R3614–3643 at different $Ca^{2+}$ concentrations by ANSA fluorescence probe. 0.5$\mu$M R4064–4210 and 2 $\mu$M ANSA was incubated in 30 mM MOPS (pH 7.2) containing 5 mM EGTA, ●; 50 $\mu$M $Ca^{2+}$, ■; 500 $\mu$M $Ca^{2+}$, ▲; or 5 mM $Ca^{2+}$, ▼ for 5 min at room temperature. Then the incubated materials were titrated with R3614–3643 and the ANSA fluorescence data were collected. $Ca^{2+}$ concentrations affect significantly the interaction of R4064–4210 with R3614–3643 (EC50 = 803 ± 47, 230 ± 7, 268 ± 8, and 181 ± 10 nM; and the Hill coefficient = 1.4 ± 0.1, 2.8 ± 0.2, 3.1 ± 0.2, and 1.9 ± 0.2 for 5 mM EGTA, 50 $\mu$M $Ca^{2+}$, 500 $\mu$M $Ca^{2+}$, and 5 mM $Ca^{2+}$, respectively).

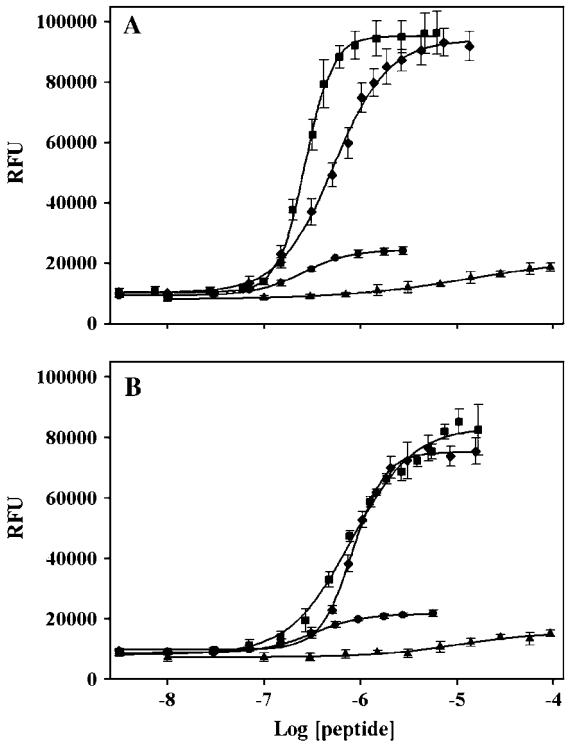


FIGURE 4 Mapping the amino acids in R3614–3643 that bind to R4064–4210. R4064–4210 (0.5 $\mu$M) and ANSA (2 $\mu$M) were incubated in 30 mM MOPS (pH 7.2) containing 500 $\mu$M $Ca^{2+}$ (*A*, high $Ca^{2+}$) or 5 mM EGTA (*B*, low $Ca^{2+}$) for 5 min at room temperature. Peptides R3614–3627, R3614–3634, R3614–3643, and R3625–3644 were added at the indicated concentrations, and the ANSA fluorescence were collected. ANSA fluorescence data in the presence of R4064–4210 per peptide were processed by subtracting the effect of R4064–4210 and peptide on the fluorescence of ANSA. (●, R3614–3634 with EC50 = 251 ± 17 nM, the Hill coefficient = 1.8 ± 0.2 for high $Ca^{2+}$ and 320 ± 21 nM, 1.7 ± 0.2 for low $Ca^{2+}$; ■, R3614–3643 with EC50 = 268 ± 8 nM, the Hill coefficient = 3.1 ± 0.2 for high $Ca^{2+}$ and 803 ± 47 nM, 1.4 ± 0.1 for low $Ca^{2+}$; ♦, R3625–3644 with EC50 = 525 ± 27 nM, the Hill coefficient = 1.5 ± 0.1 for high $Ca^{2+}$ and 835 ± 23 nM, 2.6 ± 0.2 for low $Ca^{2+}$; and ▲, R3614–3627.)

change at high $Ca^{2+}$. The R3614–3634 peptide had a higher apparent affinity for R4064–4210 (320 ± 21 nM, $n = 3$) (*solid circles* in Fig. 4 *B*) than R3614–3643 (803 ± 47 nM, $n = 3$) (*solid squares* in Fig. 4 *B*) at low $Ca^{2+}$, but again the maximal fluorescence change was much less than that produced by R3614–3643. These data suggest that the amino acids between 3635 and 3643 did not contribute greatly to the affinity but were responsible for the greater change in ANSA fluorescence with R4064–4210. A peptide corresponding to amino acids 3625–3644 produced a maximal fluorescence change comparable to R3614–3643 but with a twofold decrease in affinity ($EC_{50} = 525 \pm 27$ nM) at high $Ca^{2+}$ (*solid diamonds* in Fig. 4 *A*). The affinities of the two peptides were similar at low $Ca^{2+}$ (835 ± 23 vs. 803 ± 47 nM for 3614–3643) (*solid diamonds* in Fig. 4 *B*). A peptide corresponding to amino acids 3614–3627 (*solid up-triangles* in Fig. 4, *A* and *B*) had little effect on the ANSA fluorescence at either high or low $Ca^{2+}$ concentrations.

## Effects of R4064–4210 on ($^3$H)ryanodine binding to RyR1

If the interaction between amino acids 3614–3643 and 4064–4210 occurs within the native RyR1, and if this interaction in some way regulates the functional state of RyR1, both R4064–4210 and R3614–3643 would be predicted to modulate RyR1 activity by interfering with interactions within RyR1. To test this possibility, we examined the effects of R4064–4210 and R3614–3643 on the ($^3$H)ryanodine binding to RyR1 at different $Ca^{2+}$ concentrations. For comparison, the effects of CaM on ($^3$H)ryanodine binding are also shown.

($^3$H)Ryanodine binding is frequently used to assess functional effects on RyR1 since ryanodine preferentially binds to the open state of the channel (35). $Ca^{2+}$ titration of ($^3$H)ryanodine binding to SR membranes in the presence and absence of R4064–4210, R3614–3643, and CaM is shown in Fig. 5. ($^3$H)Ryanodine binding to SR membranes shows a bell-shaped dependence on $Ca^{2+}$ concentration similar to the $Ca^{2+}$ dependence of channel activity: binding is low at nM $Ca^{2+}$ concentrations, increases in sub-$\mu$M $Ca^{2+}$, and reaches maximum at ~10-$\mu$M $Ca^{2+}$, and then decreases (Fig. 5, *curve* with *solid circles*). Our surprising finding were that both R4064–4210 and R3614–3643 (Fig. 5, *curves* with *solid up-triangles* and *solid down-triangles*, respectively) slightly enhanced ($^3$H)ryanodine binding at <10 nM $Ca^{2+}$, inhibited ($^3$H)ryanodine at intermediate $Ca^{2+}$ and prevented $Ca^{2+}$ inhibition of ($^3$H)ryanodine binding at high $Ca^{2+}$. For comparison, CaM activates the channel at low $Ca^{2+}$ but

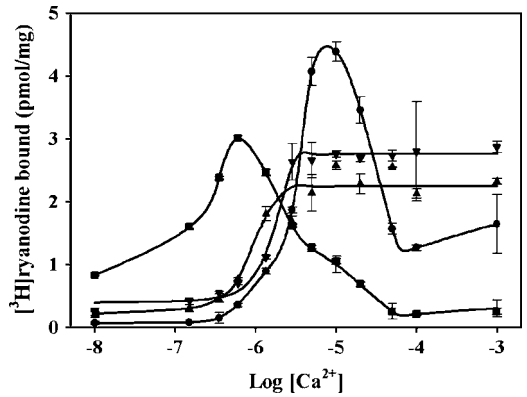


FIGURE 5 Peptides alter ($^3$H)ryanodine binding to SR membranes. SR membranes (10 $\mu$g) were incubated with 5 nM ($^3$H)ryanodine in 100 mM NaCl, 30 mM MOPS (pH 7.2) containing increasing $CaCl_2$ concentration with or without 10 $\mu$M CaM, R4064–4210, or R3614–3643 for 16 h at room temperature. The samples were filtered through Whatman GF/F filters with five washes and the radioactivity determined by liquid scintillation counting. Control, ●; CaM, ■; R4064–4210, ▲; and R3614–3643, ▼.

inhibits the channel at high $Ca^{2+}$ (Fig. 5, *curve* with *solid squares*). Since these peptides and fragments would be expected to compete with intramolecular interactions of these same sequences within RyR1, these findings suggest that an interaction between amino acids 3614–3643 and 4064–4210 within RyR1: 1), somewhat inhibits activity in low $Ca^{2+}$ (perhaps stabilizing a resting state of the channel); and 2), enhances channel activity at intermediate $Ca^{2+}$ and inhibits channel activity at high $Ca^{2+}$. CaM might activate the channel at low $Ca^{2+}$ and inhibit the channel at intermediate $Ca^{2+}$ by competing with these intramolecular interactions.

## R4064–4210 binds to CaM binding motifs

Since R4064–4210 is predicted to bind $Ca^{2+}$ and interact with CaM binding motifs within RyR1, we asked whether it could bind to other CaM binding motifs. The CaM binding sites on voltage-dependent calcium channels and RyR1 are complex sites. In both types of protein, more than one motif has been implicated in CaM binding (22,25,27–30). We examined the ability of R4064–4210 to interact with synthetic peptides representing CaM-binding motifs from these channels. Also, to determine if this is a more general protein-protein interaction motif, we assessed the ability of R4064–4210 to bind to the CaM binding peptide from CaM kinase II (aa 281–309, Calbiochem). We used changes in ANSA fluorescence in the presence of R4064–4210 to assess the interactions. We found that ANSA fluorescence in the presence of R4064–4210 increased in the presence of CaM binding peptides, R3614–3643, calmodulin kinase II inhibitor peptide (CaMKII peptide), the $Ca_V1.2$ C-peptide, and the $Ca_V1.2$ IQ-peptide (Fig. 6), suggesting that all of these peptides could bind to the CaM-like region of RyR1 and the interactions again occurs at both high and low $Ca^{2+}$ concentrations. Peptides that did not bind CaM had no effects on the ANSA fluorescence in the presence of R4064–4210 (data not shown). These interactions were confirmed by tryptophan fluorescence changes and pulldown assays with His-tagged R4064–4210 (data not shown).

## R4064–4210 binds to the $Ca_v1.1$ by pulldown analysis

If the R4064–4210 sequence can bind to the CaM binding site on $Ca_v1.1$, it should be able to pull down native $Ca_v1.1$. We tested this using His-tagged R4064–4210 and digitonin-solubilized T-tubule membranes containing the $Ca_v1.1$. Fig. 7 shows that R4064–4210 pulls down the $Ca_v1.1$ protein. Consistent with our previous findings, the pulldown of $Ca_v1.1$ by R4064–4210 does not require $Ca^{2+}$ binding to either R4064–4210 or $Ca_v1.1$ (Fig. 7 *A* for low $Ca^{2+}$ and Fig. 7 *B* for high $Ca^{2+}$). To confirm that the pulldown is specific for $Ca_v1.1$, pulldown data of Na/K ATPase by R4064–4210 are also shown in Fig. 7. At either low $Ca^{2+}$ (Fig. 7 *C*) or high $Ca^{2+}$ condition (Fig. 7 *D*), R4064–4210 does not pulldown Na/K ATPase.

## DISCUSSION

RyRs are activated by the binding of $Ca^{2+}$ at $\mu$M concentrations, but are inhibited by higher concentrations (1,2). Our data suggest that an expressed fragment containing two putative E-F hands (R4064–4210) and a synthetic peptide (R3614–3643) that represents the CaM binding motif of RyR1 interfere with an interaction that regulates the response of RyR1 to $Ca^{2+}$. These findings raise questions as to whether $Ca^{2+}$ binding to sites between amino acids 4064 and 4210 is involved in the $Ca^{2+}$ regulation of the channel and, if so, how? One possibility is that $Ca^{2+}$ binding to R4064–4210 establishes which determinants within both the 3614–3643 CaM binding site and amino acids 4064–4210 are actually interacting, and as a result, the functional outcomes of the interaction. We have previously shown that $Ca^{2+}$ binding to CaM causes an N-terminal shift in its interaction within amino acids 3614–3643 and converts CaM from an activator to an inhibitor of the channel (20,21). It is conceivable that a similar shift in the interaction of amino acids 4064–4210 with amino acids 3614–3643 could occur when $Ca^{2+}$ binds to the two sites between amino acids 4064 and 4210. It is, however, also possible that $Ca^{2+}$ binding to other sites within RYR1 alters the aa4064–4210 to aa3614–3643 interaction. The effects of R4064–4210 and R3614–3643 on the $Ca^{2+}$ dependence of ($^3$H)ryanodine binding supports the possibility that this intramolecular interaction is important for both $Ca^{2+}$ activation and inhibition of the channel. The location of the $Ca^{2+}$ activation and inhibition sites remain to be determined, but could conceivably be the two sites within amino acids 4064–4210. Scrambling the sequence of putative E-F hand 1 and E-F hand 2 within aa4064–4210 does not alter

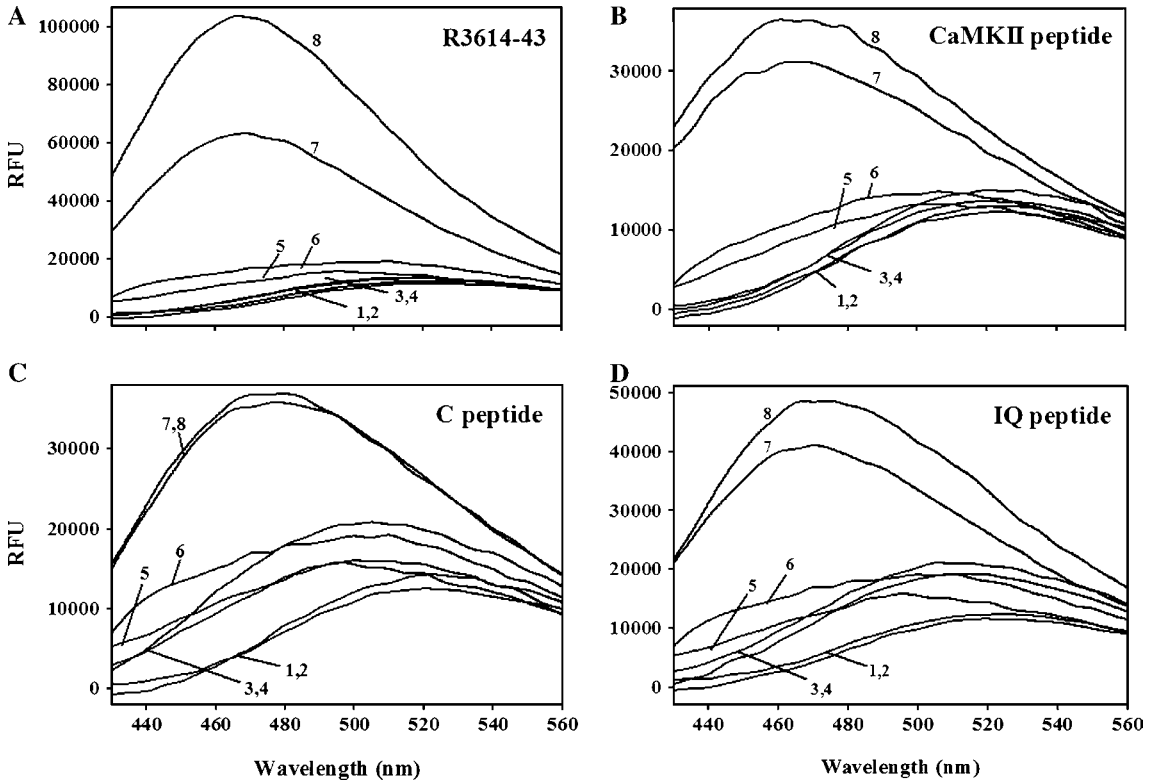


FIGURE 6 R4064–4210 binds to CaM binding motifs. R4064–4210 (0.5 $\mu$M) and ANSA (2 $\mu$M) were incubated in 30 mM MOPS (pH 7.2), 5 mM EGTA (low $Ca^{2+}$), or 500 $\mu$M $Ca^{2+}$ (high $Ca^{2+}$) for 5 min at room temperature. CaM-binding peptides (5 $\mu$M, R3614–3643 peptide, *A*; CaMKII peptide, *B*; C-peptide, *C*; and IQ-peptide, *D*) were added and ANSA fluorescence emission spectra were collected from 430 nm to 560 nm with a 370-nm excitation wavelength. (*Curve 1*, ANSA + EGTA; *curve 2*, ANSA + $Ca^{2+}$; *curve 3*, ANSA + peptide + EGTA; *curve 4*, ANSA + peptide + $Ca^{2+}$; *curve 5*, ANSA + R4064–4210 + EGTA; *curve 6*, ANSA + R4064–4210 + $Ca^{2+}$; *curve 7*, ANSA + R4064–4210 + peptide + EGTA; and *curve 8*, ANSA + R4064–4210 + peptide + $Ca^{2+}$.)

the functional responses to either depolarization or activators (caffeine or 4-CmC) when compared with wtRyR1 expressed in myotubes (19). The question is whether 4-CmC or caffeine can accurately assess alterations in the affinity of $Ca^{2+}$ activation or inhibition sites. Another question is whether the presence of endogenous CaM (which we propose competes for the interaction of aa3614–3643 with aa4064–4210) can obscure apparent changes in $Ca^{2+}$ activation or inhibition of RyR1. Fessenden et al. (36) found that RyR1 expressed in dyspedic 1B5 myotubes was activated by 4-CmC, whereas RyR3 was not. Given that RyR1 and RyR3 are both activated by $Ca^{2+}$ with only an approximately twofold difference in $Ca^{2+}$ affinity (37), but have the same apparent affinity for caffeine, one has to question whether altered responses to caffeine and 4-CmC can be used to indirectly assess RyR1 responses to $Ca^{2+}$. In addition, caffeine and 4-CmC not only increase $Ca^{2+}$ affinity of RyR1 but also alter the maximal activity. Additional data obtained by Fessenden et al. (18) with SR membranes argues that these two E-F hands play an important role in $Ca^{2+}$ regulation of the channel. Scrambling of the sequence of EF1 altered the $Ca^{2+}$ dependence of ($^3$H)ryanodine binding, with respect to both enhancement and inhibition. Even more surprisingly, scrambling of EF2 abolished high-affinity ($^3$H)ryanodine binding to membranes. Without a direct analysis of the binding of $Ca^{2+}$ to these E-F hand mutants, these studies do not rule out E-F hands 1 and 2 as sites of $Ca^{2+}$ regulation of the channel. The sequence from 4064 to 4210 binds $Ca^{2+}$ and modulates the $Ca^{2+}$ dependence of channel activity and we cannot, therefore eliminate the possibility that the $Ca^{2+}$ sites within this region are regulatory sites.

If the region containing E-F-1 and E-F-2 represents a site at which $Ca^{2+}$ regulates channel activity, the interaction of the CaM binding motif (R3614–3643) with this sequence suggests that CaM alters channel activity by interfering with these interactions in a $Ca^{2+}$-dependent fashion, activating when it is in its apoCaM form and inhibiting in its $Ca^{2+}$ bound form, both of which bind to R3614–3643. We suggest that CaM activates the channel at low $Ca^{2+}$ and inhibits the channel at intermediate $Ca^{2+}$ by competing with the intramolecular interactions between amino acids 4064–4210 and 3614–3643.

Other laboratories have also suggested that CaM might be altering RyR1 activity by interfering with an intramolecular interaction or by inducing a conformational change in the CaM binding site. Zhu et al. (38) demonstrated that a peptide

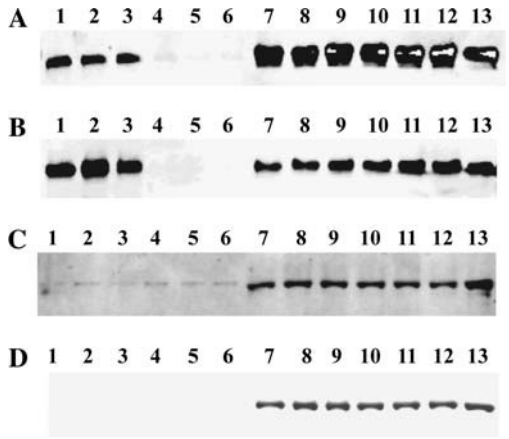


FIGURE 7 R4064–4210 binds to the native $Ca_v1.1$. His-tagged R4064–4210 or the synthetic His-tag alone were incubated with Ni-charged chelating sepharose beads and digitonin solubilized T-tubule membranes in either low, $<10$ nM $Ca^{2+}$ (*A*), or high, 1 mM $Ca^{2+}$ (*B*). After centrifugation, the pellets and supernatants were electrophoresced on 10% SDS polyacrylamide gels. After transfer to Immobilon (Millipore, Billerica, MA), the Western blots were developed with an anti-$\alpha$1 antibody from Affinity BioReagents. For comparison, Western blots were also developed with an anti-Na/K ATPase $\alpha$1 antibody, with *C* for low $Ca^{2+}$ and *D* for high $Ca^{2+}$. (*Lanes 1–3*, pulldown with His-tagged R4064–4210; *lanes 4–6*, pulldown with His tag only; *lanes 7–9*, supernatant from the pulldown with His-tagged R4064–4210; *lanes 10–12*, supernatants from the pulldowns with His-tag only; and *lane 13*, starting T-tubule preparation for the pulldown assay.)

representing the CaM binding site (amino acids 3614–3643) could either activate or inhibit RyR1, depending on the dose and the $Ca^{2+}$ concentration. They proposed that the CaM binding site was an important modulatory site within RyR1. Consistent with this, Rodney et al. (39) showed that the R3614–3643 peptide injected in frog skeletal muscle fibers increased the occurrence of $Ca^{2+}$ sparks in a dose-dependent manner, but not by displacing endogenous CaM. These studies also support the existence of an important intramolecular interaction. Gangopadhyay et al. (40) used an environment-sensitive fluorescent probe, 6-bromoacetyl-2-dimethylamino-naphthalene (badan), to study the interaction between badan-labeled calmodulin (CaM) and the CaM-binding peptide of the ryanodine receptor. They found that the interaction interface and the global conformation of the CaM-CaM binding peptide were altered by the binding of $Ca^{2+}$ to CaM.

Other amino acids are also likely to contribute to the ability of CaM to regulate RyR1 activity. Yamaguchi et al. (41) created chimeras of RyR1 and RyR2 and found that five nonconserved amino acid residues (RyR1 aa3680 and 3682–3685, and RyR2 aa3647 and 3649–3652), by differentially affecting RyR helical probability, played a key role in the ability of CaM to inhibit RyR1.

We have previously proposed that the CaM binding sequence on RyR1 can interact with determinants on the $Ca_v1.1$ and that the CaM binding sequence on the $Ca_v1.1$ can bind to determinants on RyR1 (26). We now show that the expressed fragment of RyR1 from amino acids 4064–4210 can bind to the intact $Ca_v1.1$ and to peptides representing the CaM binding sites of both RyR1 and the $Ca_v1.1$ (both the C-peptide and the IQ-peptide). We propose that the CaM binding sites on RyR1 and the $Ca_v1.1$ are more general protein-protein interaction motifs that bind to regions that contain E-F hands. The significance of this for excitation-contraction coupling is that it may provides a unique mechanism for interactions between these two ion channels: the CaM binding site on the $Ca_v1.1$ binding to the RyR1 CaM-like domain and the RyR1 CaM binding site interacting with a CaM-like domain on the $Ca_v1.1$. Since R4064–4210 of RyR1 also interacts with the CaM binding site (R3614–3643) on RyR1 to stabilize the closed channel, the interaction with the carboxyterminal tail of the $Ca_v1.1$ $\alpha_1$-subunit might disrupt an inter- or intramolecular interaction, thereby regulating RyR1 activity.

The studies were supported in part by a grant from the Muscular Dystrophy Association, and National Institutes of Health grants No. AR41802 and No. AR44864 (to S.L.H.).

## REFERENCES

1. Liu, W., D. A. Pasek, and G. Meissner. 1998. Modulation of $Ca^{2+}$-gated cardiac muscle $Ca^{2+}$-release channel (ryanodine receptor) by mono- and divalent ions. *Am. J. Physiol.* 274:C120–C128.
2. Meissner, G., E. Rios, A. Tripathy, and D. A. Pasek. 1997. Regulation of skeletal muscle $Ca^{2+}$ release channel (ryanodine receptor) by $Ca^{2+}$ and monovalent cations and anions. *J. Biol. Chem.* 272:1628–1638.
3. Kretsinger, R. H. 1976. Calcium-binding proteins. *Annu. Rev. Biochem.* 45:239–266.
4. Kretsinger, R. H. 1976. Evolution and function of calcium-binding proteins. *Int. Rev. Cytol.* 46:323–393.
5. Takeshima, H., S. Nishimura, T. Matsumoto, H. Ishida, K. Kangawa, N. Minamino, H. Matsuo, M. Ueda, M. Hanoaka, T. Hirose, and S. Numa. 1989. Primary structure and expression from complementary DNA of skeletal muscle ryanodine receptor. *Nature.* 339:439–445.
6. Nakai, J., T. Imagawa, Y. Hakamat, M. Shigekawa, H. Takeshima, and S. Numa. 1990. Primary structure and functional expression from cDNA of the cardiac ryanodine receptor/calcium release channel. *FEBS Lett.* 271:169–177.
7. Hakamata, Y., J. Nakai, H. Takeshima, and K. Imoto. 1992. Primary structure and distribution of a novel ryanodine receptor/calcium release channel from rabbit brain. *FEBS Lett.* 312:229–235.
8. Treves, S., P. Chiozzi, and F. Zorzato. 1993. Identification of the domain recognized by anti-(ryanodine receptor) antibodies which affect $Ca^{2+}$-induced $Ca^{2+}$ release. *Biochem. J.* 291:757–763.
9. Chen, S. R., L. Zhang, and D. H. MacLennan. 1992. Characterization of a $Ca^{2+}$ binding and regulatory site in the $Ca^{2+}$ release channel (ryanodine receptor) of rabbit skeletal muscle sarcoplasmic reticulum. *J. Biol. Chem.* 267:23318–23326.
10. Chen, S. R., L. Zhang, and D. H. MacLennan. 1993. Antibodies as probes for $Ca^{2+}$ activation sites in the $Ca^{2+}$ release channel (ryanodine receptor) of rabbit skeletal muscle sarcoplasmic reticulum. *J. Biol. Chem.* 268:13414–13421.
11. Zorzato, F., J. Fujii, K. Otsu, M. Phillips, N. M. Green, F. A. Lai, G. Meissner, and D. H. MacLennan. 1990. Molecular cloning of cDNA encoding human and rabbit forms of the $Ca^{2+}$ release channel (ryanodine receptor) of skeletal muscle sarcoplasmic reticulum. *J. Biol. Chem.* 265:2244–2256.
12. Hayek, S. M., X. Zhu, M. B. Bhat, J. Zhao, H. Takeshima, H. H. Valdivia, and J. Ma. 2000. Characterization of a calcium-regulation

domain of the skeletal-muscle ryanodine receptor. *Biochem. J.* 351: 57–65.

13. Du, G. G. and D. H. MacLennan. 1999. $Ca^{2+}$ inactivation sites are located in the COOH-terminal quarter of recombinant rabbit skeletal muscle Ca(2+) release channels (ryanodine receptors). *J. Biol. Chem.* 274:26120–26126.
14. Chen, S. R. W., and D. H. MacLennan. 1994. Identification of calmodulin, $Ca^{2+}$, and ruthenium red-binding domains in the $Ca^{2+}$ release channel (ryanodine receptor) of rabbit skeletal muscle sarcoplasmic reticulum. *J. Biol. Chem.* 269:22698–22704.
15. Xiong, H., X. Feng, L. Gao, L. Xu, D. A. Pasek, J. H. Seok, and G. Meissner. 1998. Identification of a two EF-hand $Ca^{2+}$ binding domain in lobster skeletal muscle ryanodine receptor/$Ca^{2+}$ release channel. *Biochemistry.* 37:4804–4814.
16. Hamada, T., Y. Sakube, J. Ahnn, H. Kim, and H. Kagawa. 2002. Molecular dissection, tissue localization and $Ca^{2+}$ binding of the ryanodine receptor of Caenorhabditis elegans. *J. Mol. Biol.* 324:123–135.
17. Fessenden, J. D., L. Chen, Y. Wang, C. Paolini, C. Franzini-Armstrong, P. D. Allen, and I. N. Pessah. 2001. Ryanodine receptor point mutant E4032A reveals an allosteric interaction with ryanodine. *Proc. Natl. Acad. Sci. USA.* 98:2865–2870.
18. Fessenden, J. D., W. Feng, I. N. Pessah, and P. D. Allen. 2004. Mutational analysis of putative calcium binding motifs within the skeletal ryanodine receptor isoform, RyR1. *J. Biol. Chem.* 279:53028–53035.
19. Tripathy, A., L. Xu, G. Mann, and G. Meissner. 1995. Calmodulin activation and inhibition of skeletal muscle $Ca^{2+}$ release channel (ryanodine receptor). *Biophys. J.* 69:106–119.
20. Rodney, G. G., B. Y. Williams, G. M. Strasburg, K. Beckingham, and S. L. Hamilton. 2000. Regulation of RyR1 activity by $Ca^{2+}$ and calmodulin. *Biochemistry.* 39:7807–7812.
21. Rodney, G. G., C. P. Moore, B. Y. Williams, J. Z. Zhang, J. Krol, S. E. Pedersen, and S. L. Hamilton. 2001. Calcium binding to calmodulin leads to an N-terminal shift in its binding site on the ryanodine receptor. *J. Biol. Chem.* 276:2069–2074.
22. Moore, C. P., J.-Z. Zhang, and S. L. Hamilton. 1999. A role for Cysteine 3635 of RyR1 in redox modulation and calmodulin binding. *J. Biol. Chem.* 274:36831–36834.
23. Rodney, G. G., J. Krol, B. Williams, K. Beckingham, and S. L. Hamilton. 2001. The carboxy-terminal calcium binding sites of calmodulin control calmodulin's switch from an activator to an inhibitor of RyR1. *Biochemistry.* 40:12430–12435.
24. Xiong, L. W., R. A. Newman, G. G. Rodney, O. Thomas, J. Z. Zhang, A. Persechini, M. A. Shea, and S. L. Hamilton. 2002. Lobe-dependent regulation of ryanodine receptor Type 1 by calmodulin. *J. Biol. Chem.* 277:40862–40870.
25. Zhang, H., J. Z. Zhang, C. I. Danila, S. L. Hamilton, and A. Noncontiguous. 2003. Inter-subunit binding site for calmodulin on the skeletal muscle $Ca^{2+}$ release channel. *J. Biol. Chem.* 278:8348–8355.
26. Sencer, S., R. V. Papineni, D. B. Halling, P. Pate, J. Krol, J. Z. Zhang, and S. L. Hamilton. 2001. Coupling of RyR1 and L-type calcium channels via calmodulin binding domains. *J. Biol. Chem.* 276:38237–38241.
27. Pate, P., J. Mochca-Morales, Y. Wu, J. Z. Zhang, G. G. Rodney, I. I. Serysheva, B. Y. Williams, M. E. Anderson, and S. L. Hamilton. 2000. Determinants for calmodulin binding on voltage-dependent $Ca^{2+}$ channels. *J. Biol. Chem.* 275:39786–39792.
28. Pitt, G. S., R. D. Zuhlke, A. Hudmon, H. Schulman, H. Reuter, and R. W. Tsien. 2001. Molecular basis of calmodulin tethering and $Ca^{2+}$-dependent inactivation of L-type $Ca^{2+}$ channels. *J. Biol. Chem.* 276: 30794–30802.
29. Soldatov, N. M., M. Oz, K. A. O'Brien, D. R. Abernethy, and M. Morad. 1998. Molecular determinants of L-type $Ca^{2+}$ channel inactivation. segment exchange analysis of the carboxyl-terminal cytoplasmic motif encoded by exons 40–42 of the human $\alpha$1C-subunit gene. *J. Biol. Chem.* 273:957–963.
30. Zühlke, R. D., and H. Reuter. 1998. $Ca^{2+}$-sensitive inactivation of L-type $Ca^{2+}$ channels depends on multiple cytoplasmic amino acid sequences of the $\alpha$1C-subunit. *Proc. Natl. Acad. Sci. USA.* 95:3287–3294.
31. Hawkes, M. J., M. Díaz-Muñoz, and S. L. Hamilton. 1989. A procedure for the purification of the ryanodine receptor from skeletal muscle. *Membr. Biochem.* 8:133–145.
32. Lowry, O. H., N. J. Rosebrough, A. L. Farr, and R. J. Randall. 1951. Protein measurement with the folin phenol reagent. *J. Biol. Chem.* 193:265–275.
33. Venyaminov, S. Y., and J. T. Yang. 1996. Circular Dichroism and the Conformational Analysis of Biomolecules. G. D. Fasman, editor. Plenum Publishing, New York. 69–108.
34. Muesing, R. A., and T. Nishida. 1971. Disruption of low- and high-density human plasma lipoproteins and phospholipid dispersions by 1-anilinonaphthalene-8-sulfonate. *Biochemistry.* 10:2952–2962.
35. Chu, A., M. Diaz-Munoz, M. J. Hawkes, K. Brush, and S. L. Hamilton. 1990. Ryanodine as a probe for the functional state of the skeletal muscle sarcoplasmic reticulum $Ca^{2+}$ release channel. *Mol. Pharmacol.* 37:735–741.
36. Fessenden, J. D., C. F. Perez, S. Goth, I. N. Pessah, and P. D. Allen. 2003. Identification of a key determinant of ryanodine receptor Type 1 required for activation by 4-chloro-m-cresol. *J. Biol. Chem.* 278: 28727–28735.
37. Murayama, T., and Y. Ogawa. 2004. RyR1 exhibits lower gain of CICR activity than RyR3 in the SR: evidence for selective stabilization of RyR1 channel. *Am. J. Physiol. Cell Physiol.* 287:C36–C45.
38. Zhu, X., J. Ghanta, J. W. Walker, P. D. Allen, and H. H. Valdivia. 2004. The calmodulin binding region of the skeletal ryanodine receptor acts as a self-modulatory domain. *Cell Calcium.* 35:165–177.
39. Rodney, G. G., G. M. Wilson, and M. F. Schneider. 2005. A calmodulin binding domain of RyR increases activation of spontaneous $Ca^{2+}$ sparks in frog skeletal muscle. *J. Biol. Chem.* 280:11713–11722.
40. Gangopadhyay, J. P., Z. Grabarek, and N. Ikemoto. 2004. Fluorescence probe study of $Ca^{2+}$-dependent interactions of calmodulin with calmodulin-binding peptides of the ryanodine receptor. *Biochem. Biophys. Res. Commun.* 323:760–768.
41. Yamaguchi, N., L. Xu, K. E. Evans, D. A. Pasek, and G. Meissner. 2004. Different regions in skeletal and cardiac muscle ryanodine receptors are involved in transducing the functional effects of calmodulin. *J. Biol. Chem.* 279:36433–36439.